Tokyo Climate Center, Japan Meteorological Agency

TCC News

Spring 2023

Table of Contents: TCC News No. 72

El Niño Outlook (May - November 2023) 1
JMA's Seasonal Numerical Ensemble Prediction for Boreal Summer 2023 3
Summary of the 2022/2023 Asian Winter Monsoon 6
Commencement of JRA-3Q utilization in diagnosis products and iTacs 12
TCC and WMC Tokyo co-contributions to Regional Climate Outlook Forums 14

El Niño Outlook (May - November 2023)

Atmospheric and oceanic indicators suggest that ENSO-neutral conditions continued in April, while the situation in the equatorial Pacific evolved toward El Niño characteristics. It is likely that El Niño conditions will develop by boreal summer (80%) (article based on the El Niño outlook issued on 12 May 2023).

1. El Niño/La Niña

In April 2023, the sea surface temperature (SST) for the NINO.3 region was above normal with a deviation of +0.5°C. SSTs were above normal in western and eastern parts of the equatorial Pacific (Figures 1-1 and 1-3 (a)), while subsurface temperatures were above-normal in most parts (Figures 1-2 and 1-3 (b)). In the atmosphere, convective activity near the date line over the equatorial Pacific was below normal, and easterly winds in the lower troposphere (i.e., trade winds) over central parts were near normal. These patterns indicate that ENSO-neutral conditions continued in April, while the situation in the equatorial Pacific evolved toward El Niño characteristics.

The warm subsurface water volume in central and eastern parts of equatorial Pacific (Figure 1-2) maintained higher SST in the NINO.3 region. JMA's seasonal ensemble prediction system forecasts that this volume will be warmer and exhibit higher SSTs in the eastern part, and that NINO.3 SSTs will be above normal during the prediction period (Figure 1-4). In conclusion, it is likely that El Niño conditions will develop by boreal summer (80%) (Figure 1-5).

2. Western Pacific and Indian Ocean

The area-averaged SST in the tropical western Pacific (NINO.WEST) region was above normal in April. The index is likely to be near or below normal in boreal summer.

The area-averaged SST in the tropical Indian Ocean (IOBW) region was near normal in April. The index is likely to be near normal until boreal summer.

(SATO Hirotaka, Tokyo Climate Center)

* The SST normal for the NINO.3 region (5°S – 5°N, 150°W – 90°W) is defined as a monthly average over the latest sliding 30-year period (1993-2022 for this year).

* The SST normals for the NINO.WEST region (Eq. – 15°N, 130°E – 150°E) and the IOBW region (20°S – 20°N, 40°E – 100°E) are defined as linear extrapolations with respect to the latest sliding 30-year period, in order to remove the effects of significant long-term warming trends observed in these regions.

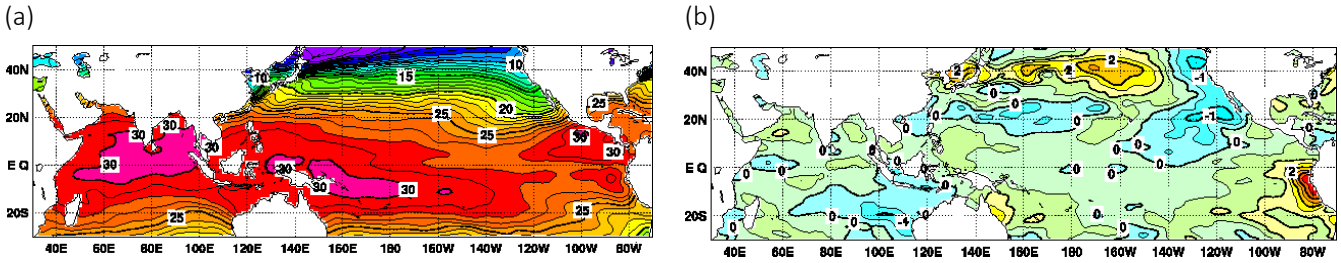

Figure 1-1 Monthly mean (a) sea surface temperatures (SSTs) and (b) SST anomalies in the Indian and Pacific Ocean areas for April 2023
The contour intervals are 1°C in (a) and 0.5°C in (b). The base period for the normal is 1991 – 2020.

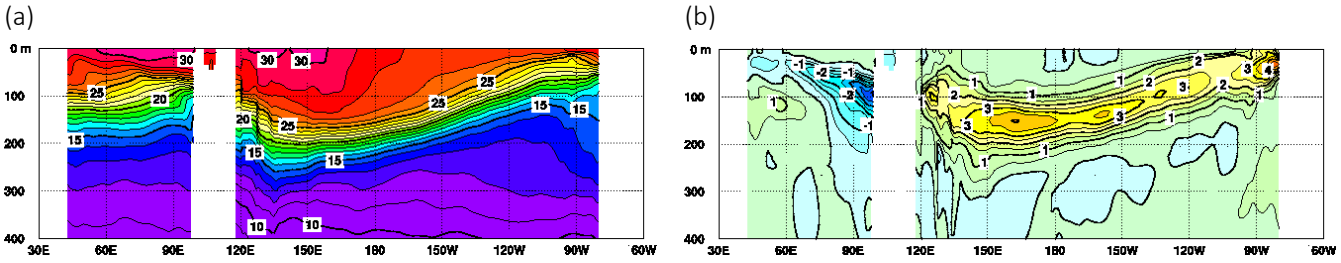

Figure 1-2 Monthly mean depth-longitude cross sections of (a) temperatures and (b) temperature anomalies in the equatorial Indian and Pacific Ocean areas for April 2023
The contour intervals are 1°C in (a) and 0.5°C in (b). The base period for the normal is 1991 – 2020.

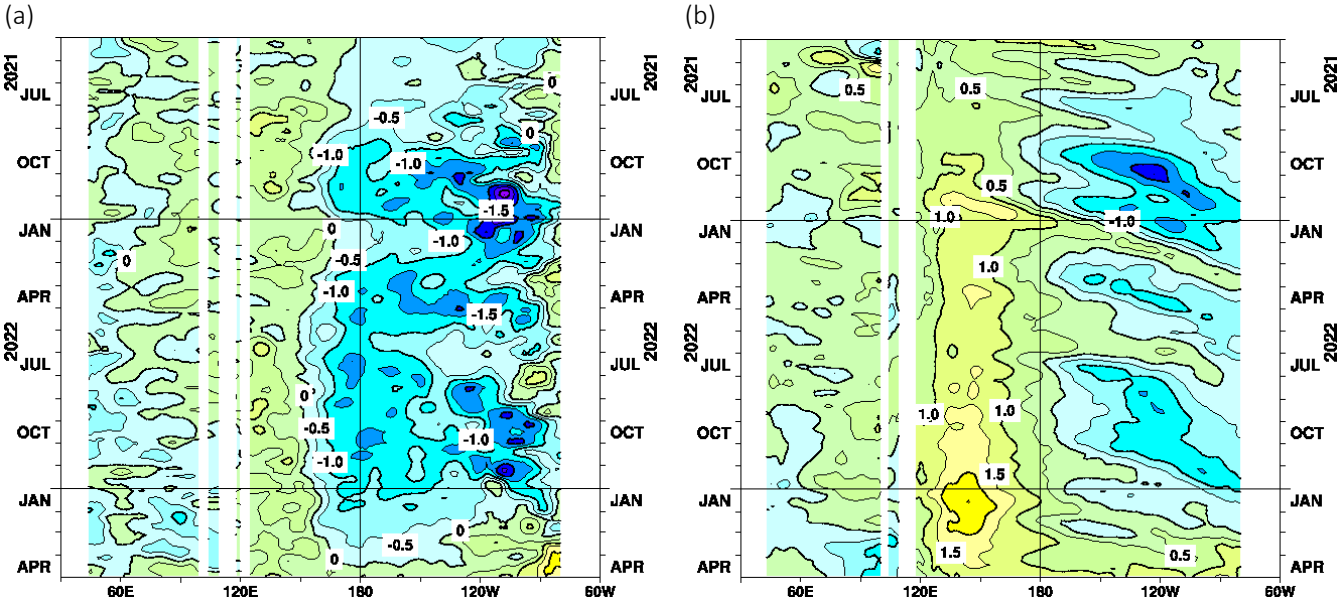

Figure 1-3 Time-longitude cross sections of (a) SST and (b) ocean heat content (OHC) anomalies along the equator in the Indian and Pacific Ocean areas
OHCs are defined here as vertically averaged temperatures in the top 300 m. The base period for the normal is 1991 – 2020.

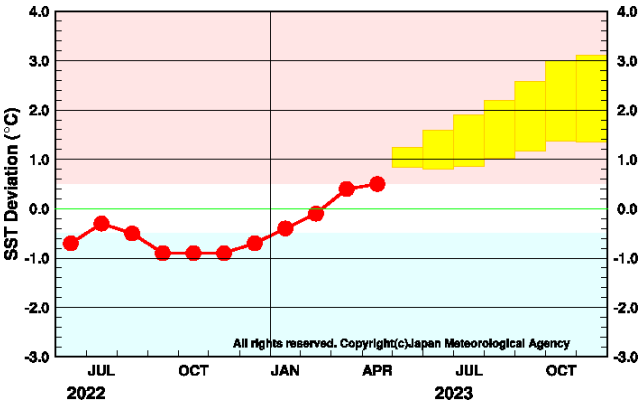

Figure 1-4 Outlook of NINO.3 SST deviation produced by the seasonal ensemble prediction system

This figure shows a time series of monthly NINO.3 SST deviations. The thick line with closed circles shows observed SST deviations, and the boxes show the values produced for up to six months ahead by the seasonal ensemble prediction system. Each box denotes the range into which the SST deviation is expected to fall with a probability of 70%.

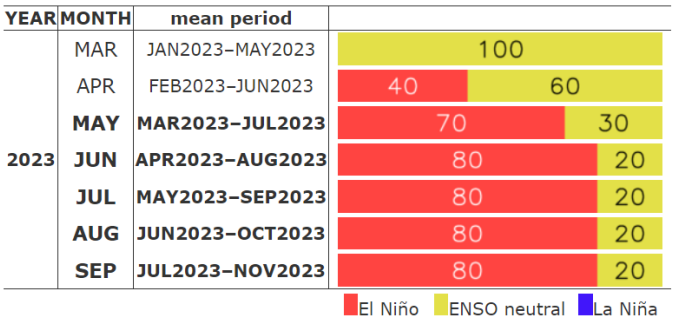

Figure 1-5 ENSO forecast probabilities based on the seasonal ensemble prediction system

Red, yellow and blue bars indicate probabilities that the five-month running mean of the NINO.3 SST deviation from the latest sliding 30-year mean will be +0.5°C or above (El Niño), between +0.4 and -0.4°C (ENSO-neutral) and -0.5°C or below (La Niña), respectively. Regular text indicates past months, and bold text indicates current and future months.

<<Table of contents <Top of this article

JMA's Seasonal Numerical Ensemble Prediction for Boreal Summer 2023

This report outlines JMA's dynamical seasonal ensemble prediction for boreal summer 2023 (June – August, referred to as JJA), which was used as a basis for JMA's operational three-month outlook issued on 23 May 2023. The outlook is based on the seasonal ensemble prediction system of the Coupled Atmosphere-ocean General Circulation Model (CGCM).

Summary: ENSO-neutral conditions continued in April, and it is likely that El Niño conditions will develop by boreal summer. In association with above-normal SSTs from the equatorial Pacific to the area around the Maritime Continent, enhanced convection is expected from the Bay of Bengal to the western equatorial Pacific. In the lower troposphere, cyclonic circulation anomalies straddling the equator are expected near the Maritime Continent and in central to eastern parts of the tropical Pacific.

1. Sea surface temperatures

Figure 2-1 shows predicted SSTs (contours) and related anomalies (shading) for JJA. Positive anomalies are expected from the equatorial Pacific to the area around the Maritime Continent. Subsurface warm waters observed in the central part of the equatorial Pacific are expected to migrate eastward and cause increased SSTs in the eastern part in boreal summer, although there is significant uncertainty regarding the degree to which this will affect NINO.3 SSTs. JMA's seasonal ensemble prediction system forecasts that NINO.3 SSTs will rise to above normal in boreal summer. In conclusion, it is likely that El Niño conditions will develop by boreal summer (80%). In the tropical Indian Ocean, positive anomalies in the western part and negative anomalies in central and eastern parts are expected in boreal summer.

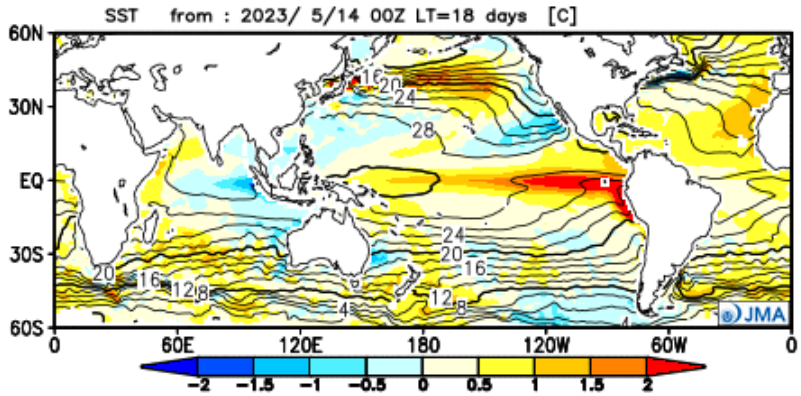

Figure 2-1 Predicted SSTs (contours) and SST anomalies (shading) for June–August 2023 (ensemble mean of 51 members)

2. Prediction for the tropics and sub-tropics

Figure 2-2 (a) shows predicted precipitation (contours) and related anomalies (shading) for JJA. Precipitation is expected to be above normal from the Bay of Bengal to the western equatorial Pacific and below normal over and around the equatorial Indian Ocean.

Figure 2-2 (b) shows predicted velocity potential (contours) and related anomalies (shading) in the upper troposphere for JJA. In association with the precipitation anomalies described above, large-scale divergence and convergence anomalies are expected over the western tropical Pacific and the Indian Ocean, respectively.

Figure 2-2 (c) shows predicted stream functions (contours) and related anomalies (shading) in the upper troposphere for JJA. Anti-cyclonic circulation anomalies straddling the equator are expected near the Maritime Continent and over central to eastern parts of the tropical Pacific, and cyclonic circulation anomalies straddling the equator are expected from the tropical Atlantic to Africa.

Figure 2-2 (d) shows predicted stream functions (contours) and related anomalies (shading) in the lower troposphere for JJA. Cyclonic (i.e., negative in the Northern Hemisphere) circulation anomalies straddling the equator are expected near the Maritime Continent and central to eastern parts of the tropical Pacific.

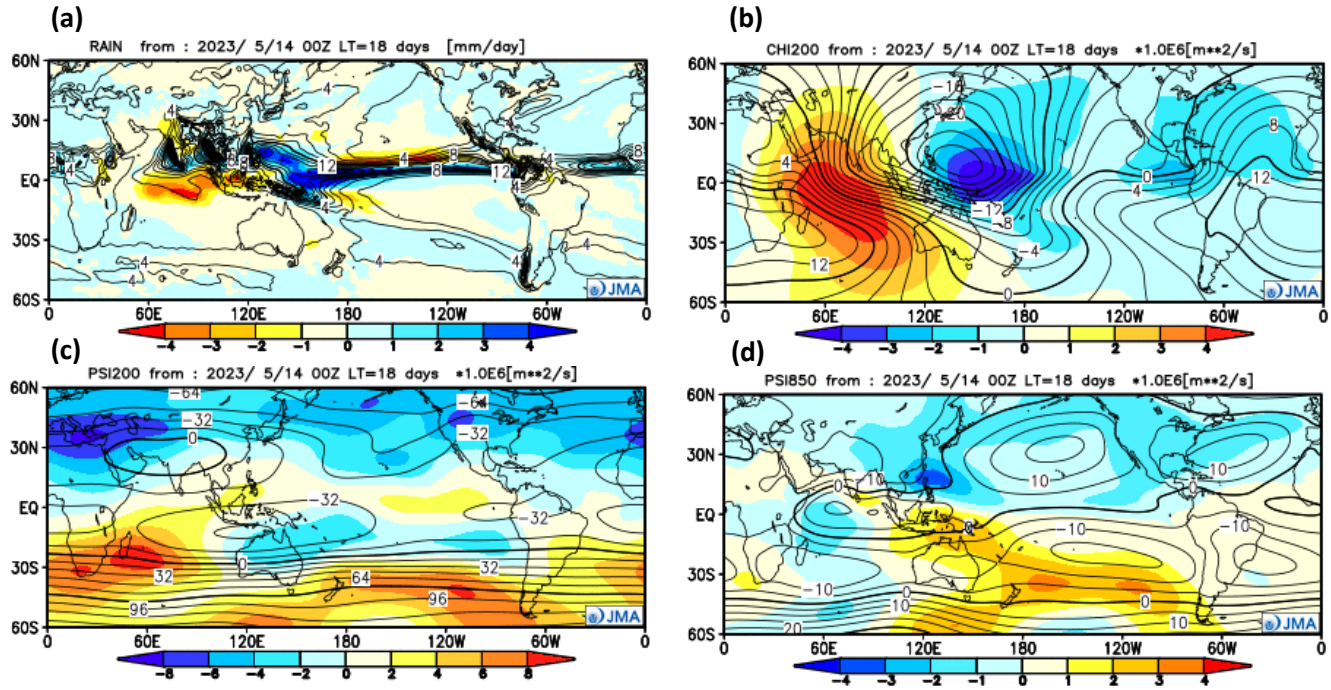

Figure 2-2 Predicted atmospheric fields over 60°N-60°S for June–August 2023 (ensemble mean of 51 members)
(a) Precipitation (contours) and anomaly (shading). The contour interval is 2 mm/day. (b) Velocity potential at 200-hPa (contours) and anomaly (shading). The contour interval is 2 × 10^6 m^2/s. (c) Stream function at 200-hPa (contours) and anomaly (shading). The contour interval is 16 × 10^6 m^2/s. (d) Stream function at 850-hPa (contours) and anomaly (shading). The contour interval is 5 × 10^6 m^2/s.

3. Prediction for the mid- and high- latitudes of the Northern Hemisphere

Figure 2-3 (a) shows predicted 500-hPa geopotential heights (contours) and related anomalies (shading) for JJA. Positive anomalies are expected over a wide area of the Northern Hemisphere.

Figure 2-3 (b) shows predicted sea level pressure (contours) and related anomalies (shading) for JJA. Positive anomalies are expected from East Asia to the sea southeast of Japan, and negative anomalies are expected over the subtropical western North Pacific and the eastern North Pacific.

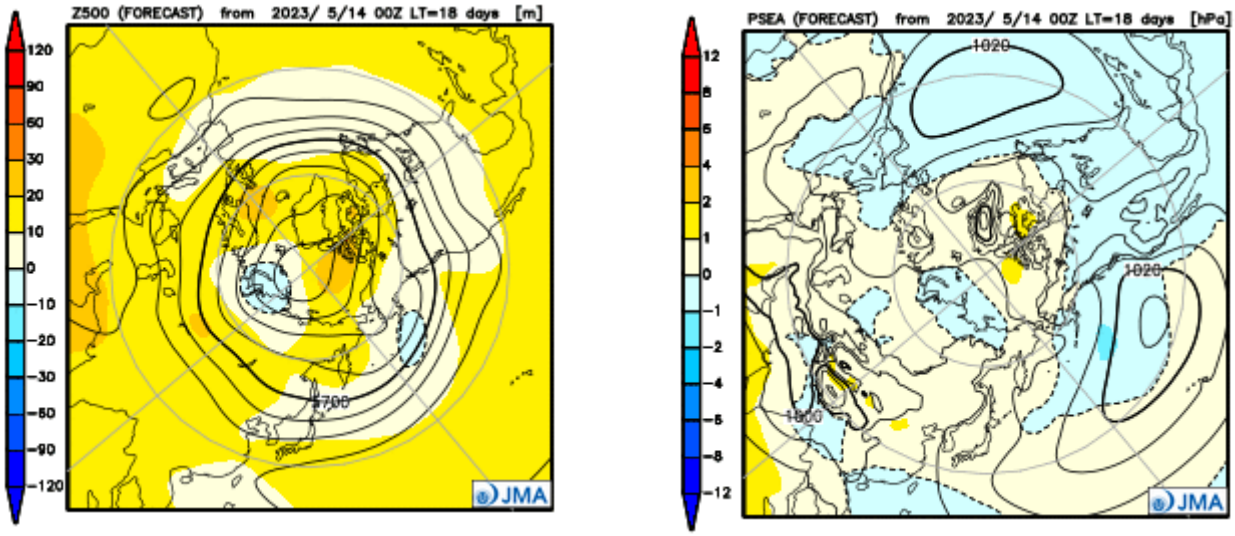

Figure 2-3 Predicted atmospheric fields over 20°N-90°N for June–August 2023 (ensemble mean of 51 members)
(a) Geopotential height at 500-hPa (contours) and anomaly (shading). The contour interval is 60 m. (b) Sea level pressure (contours) and anomaly (shading). The contour interval is 4 hPa.

Note: JMA operates a seasonal Ensemble Prediction System (EPS) using the Coupled atmosphere-ocean General Circulation Model (CGCM) to make seasonal predictions beyond a one-month time range. The EPS produces perturbed initial conditions by means of a combination of the initial perturbation method and the lagged average forecasting (LAF) method. Prediction is made using 51 members from the latest 17 initial dates (3 members are used every day). Details of the prediction system and verification maps based on 30-year hindcast experiments (1991–2020) are available at https://ds.data.jma.go.jp/tcc/tcc/products/model/.

(ITO Akira, Tokyo Climate Center)

<<Table of contents <Top of this article

Summary of the 2022/2023 Asian Winter Monsoon

This report summarizes the characteristics of the surface climate and atmospheric/oceanographic conditions related to the Asian winter monsoon for 2022/2023.

Note: Dataset of the Japanese Reanalysis for Three Quarters of a century (JRA-3Q) (Kobayashi et al. 2021) and MGDSST (Kurihara et al. 2006) were used to analyze atmospheric circulation and sea surface temperature (SST). NOAA Interpolated Outgoing Longwave Radiation (OLR) data (Liebmann and Smith 1996) provided by the U.S. NOAA Physical Sciences Laboratory (PSL) from their web site at https://psl.noaa.gov/data/gridded/data.interp_OLR.html was used to infer tropical convective activity. The base period for the normal is 1991 to 2020. The term “anomaly” as used in this report refers to deviation from the normal.

1. Surface climate conditions

In winter 2022/2023, three-month (DJF) mean temperatures were near normal over most of East Asia and below normal from the western part of Eastern Siberia to northern Japan (Figure 3-1 (a)) although notable monthly temperature variations were observed. Below-normal temperature anomalies indicative of extreme cold spells were seen over most of East Asia in December (Figure 3-1 (b)) and from Central Siberia to northern Japan in January (Figure 3-1 (c)) corresponding to a stronger-than-normal East Asian Winter Monsoon (EAWM), in contrast to the East Asia-wide warm anomalies seen in February (Figure 3-1 (d)). Winter precipitation amounts were above normal in and around Southeast Asia (Figure 3-2).

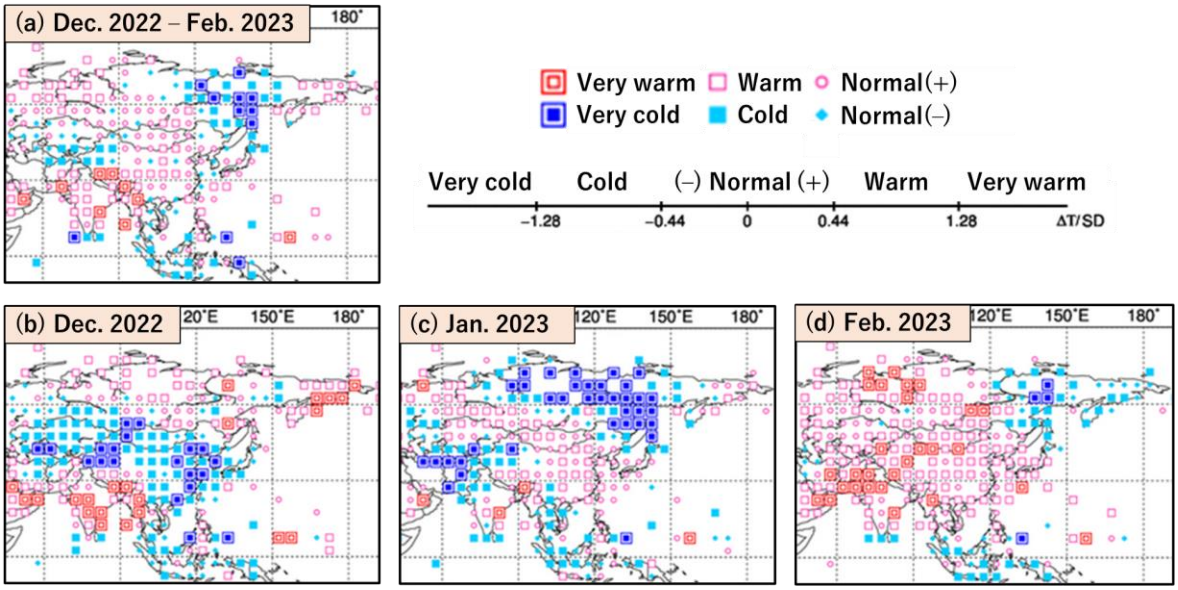

Figure 3-1 Temperature anomalies for (a) December 2022 to February 2023, (b) December 2022, (c) January 2023 and (d) February 2023

Categories are defined by the three-month/monthly mean temperature anomaly against the normal divided by its standard deviation and averaged in 5° × 5° grid boxes. The thresholds of each category are –1.28, –0.44, 0, +0.44 and +1.28. Standard deviations were calculated from 1991 – 2020 statistics. Areas over land without graphical marks are those where observation data are insufficient or where normal data are unavailable.

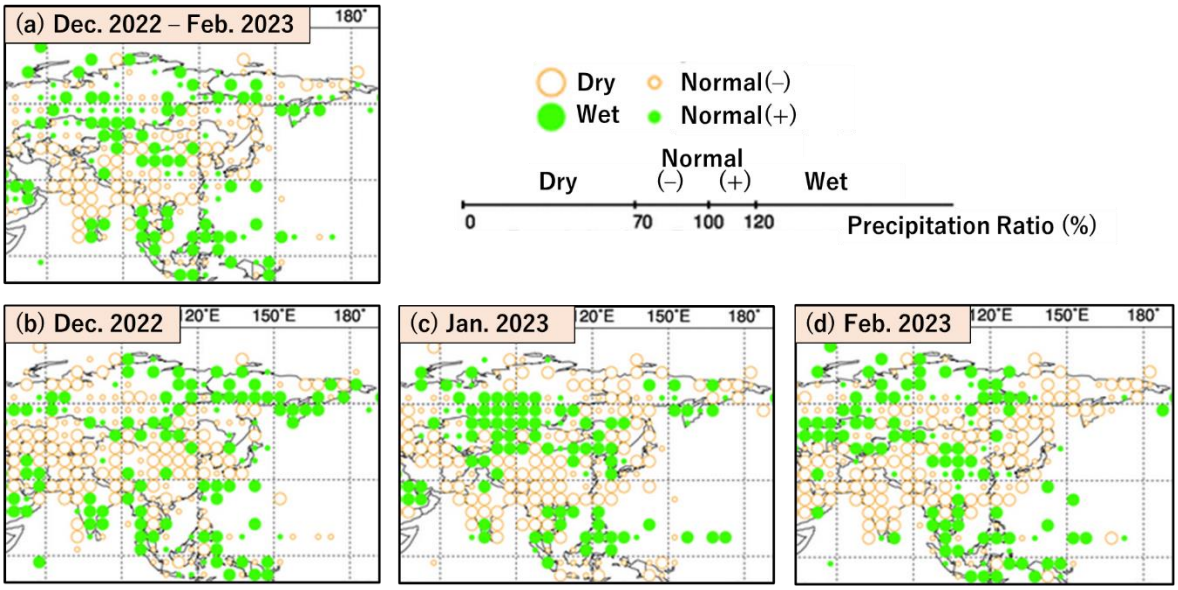

Figure 3-2 Precipitation ratio for (a) December 2022 to February 2023, (b) December 2022, (c) January 2023 and (d) February 2023

Categories are defined by the three-month/monthly precipitation ratio against the normal and averaged in 5° × 5° grid boxes. The thresholds of each category are 70, 100 and 120%. Areas over land without graphical marks are those where observation data are insufficient or where normal data are unavailable.

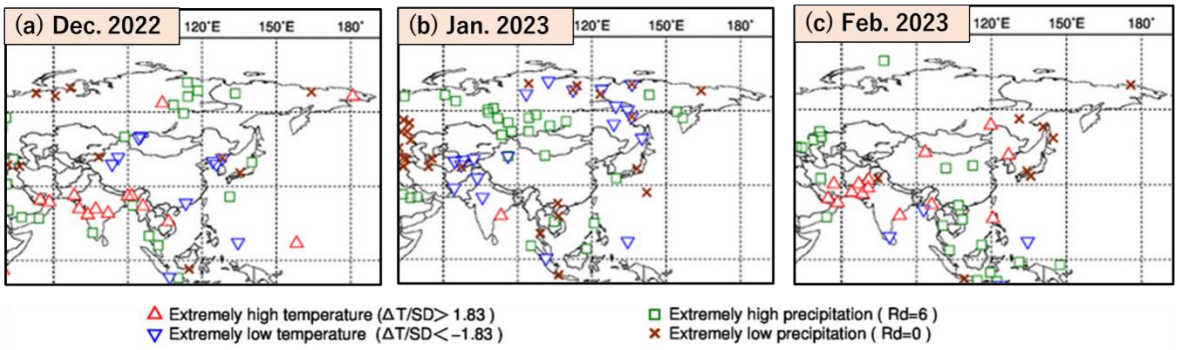

Figure 3-3 Extreme climate stations for (a) December 2022, (b) January 2023 and (c) February 2023
ΔT, SD and Rd indicate temperature anomaly, standard deviation and quintile, respectively.

Figure 3-3 plots stations where extreme climatic conditions were observed between December 2022 and February 2023. Extremely low temperatures were seen from the central part of Central Siberia to the southwestern part of Eastern Siberia in January (Figure 3-3 (b); see also Figure 3-1 (c)). Extremely high precipitation amounts were seen in parts of Southeast Asia, especially over eastern Indonesia in February (Figure 3-3 (c)).

2. Characteristic atmospheric circulation and oceanographic conditions

This section presents characteristics of atmospheric circulation and oceanographic conditions averaged in winter 2022/2023.

2.1 Conditions in the tropics

Figure 3-4 shows three-month winter mean SST anomalies and anomalous convective activity. Values are negative from the central to the eastern equatorial Pacific and positive over the tropical western North Pacific (Figure 3-4 (a)) in association with the La Niña event that began in boreal autumn 2021 and ended during the winter in question. Negative SST anomalies were observed in the eastern part of the tropical Indian Ocean (Figure 3-4 (a)), while convective activity inferred from OLR was enhanced from the eastern Indian Ocean to Southeast Asia and suppressed near the date line in the equatorial Pacific (Figure 3-4 (b)) in association with La Niña-related SST anomalies (Figure 3-4 (a)). In the upper troposphere, large-scale divergence anomalies were dominant over and around the Maritime Continent, and large-scale convergence anomalies were seen near the date line in the equatorial Pacific in association with tropical convection anomalies (Figure 3-4 (b)). The large-scale anomalous divergence promoted northward divergent winds in the area from the Maritime Continent to East Asia, partly contributing to northward meandering of the subtropical jet stream (STJ) as described later.

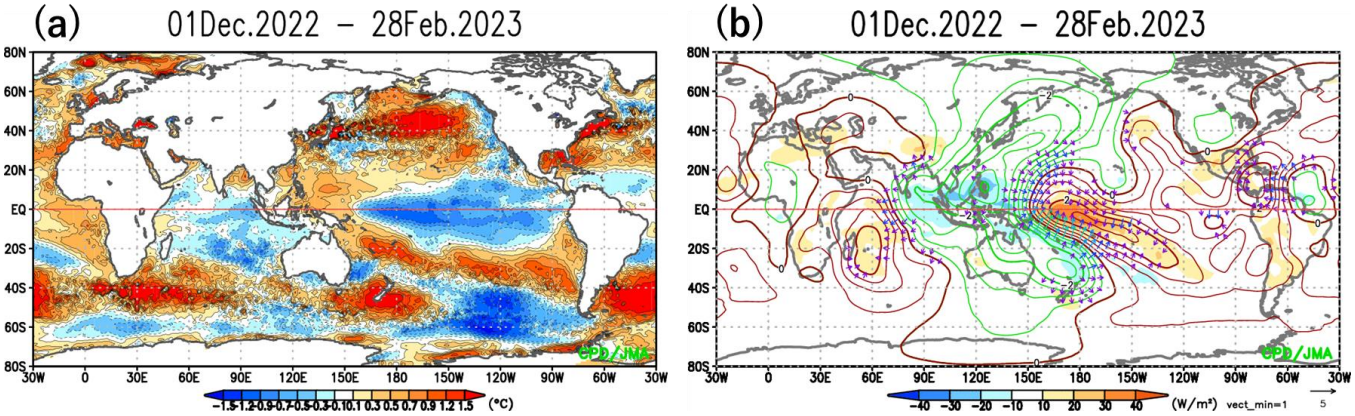

Figure 3-4 Three-month mean (a) SST anomalies and (b) anomalous convective activity in winter 2022/2023

The shadings in (a) and (b) show the SST anomalies [°C] and OLR anomalies [W/m^2]. The contours and vectors in (b) indicate 200-hPa velocity potential anomalies at intervals of 0.5 × 10^6 m^2/s and divergent wind anomalies, respectively. Negative (cold color) and positive (warm color) OLR anomalies show enhanced and suppressed convective activity compared to the normal, respectively.

Figure 3-5 shows three-month mean 200 and 850-hPa stream function anomalies for winter. In the upper troposphere, anti-cyclonic circulation anomalies were seen from South Asia to the sea south of Japan (Figure 3-5 (a)), corresponding to the northward shift of the STJ from its normal position from eastern Eurasia to the sea east of Japan. These anomalies are partly attributable to enhanced convection in the area from the eastern Indian Ocean to Southeast Asia, as evidenced by a numerical experiment using a linear baroclinic model (Watanabe and Kimoto 2000, 2001) and vorticity budget analysis (not shown). In the central tropical Pacific, cyclonic circulation anomalies straddling the equator were seen in response to suppressed convection in the area near the date line in the equatorial Pacific (Figure 3-5 (a)). In the lower troposphere, circulation anomalies straddling the equator (as per those in the upper troposphere, but with the sign reversed) were seen in the area from the Indian Ocean to the central tropical Pacific (Figure 3-5 (b)).

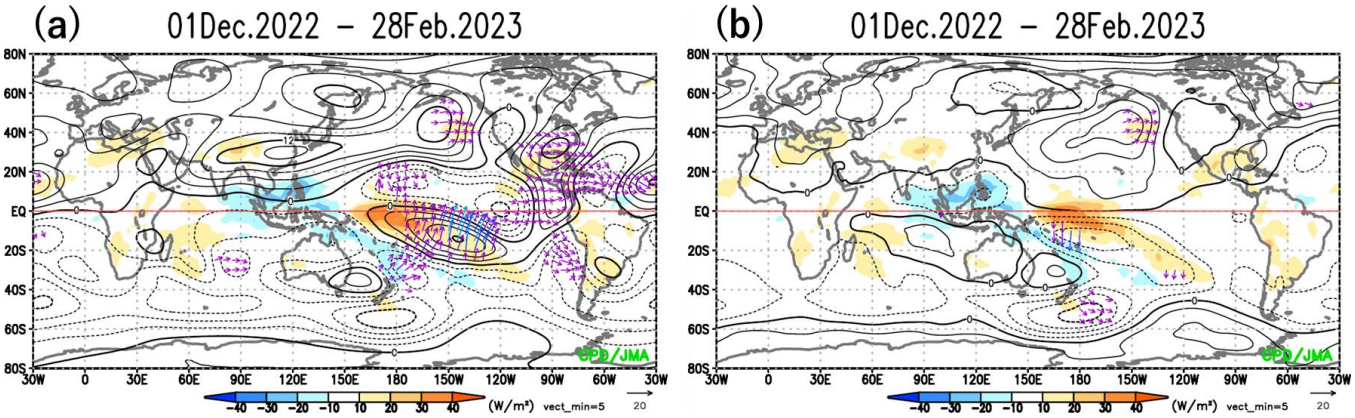

Figure 3-5 Three-month mean (a) 200-hPa and (b) 850-hPa stream function anomalies in winter 2022/2023

The contours indicate stream function anomalies at intervals of (a) 3 × 10^6 m^2/s and (b) 1.5 × 10^6 m^2/s, and the shadings show OLR anomalies [W/m^2]. The vectors denote horizontal component of wave activity flux [m^2/s^2] defined by Takaya and Nakamura (2001).

2.2 Conditions in the extratropics

Figure 3-6 shows three-month mean 500-hPa height, sea level pressure and 850-hPa temperature in the Northern Hemisphere. In the 500-hPa height field (Figure 3-6 (a)), the tropospheric polar vortex (usually located over the Arctic region) split in association with positive anomalies over the northern polar region and negative anomalies in the area from Eastern Siberia to the northern part of East Asia. The positive height anomalies imply frequent appearance of blocking highs over the sea north of Eastern Siberia. Wave trains of height anomalies as seen in the positive phase of the Eurasian teleconnection pattern (Wallace and Gutzler 1981) were seen over northern Eurasia. These conditions indicate a tendency for the polar front jet stream (PFJ) to meander southward over East Asia. Lower-level temperatures were below normal in the area from Central/Eastern Siberia to northern East Asia (Figure 3-6 (c)) in association with the negative 500-hPa height anomalies described above (Figure 3-6 (a)). In the sea level pressure field (Figure 3-6 (b)), the Siberian High was stronger than normal from central to western parts, and the Aleutian Low was stronger than normal in the northwestern part.

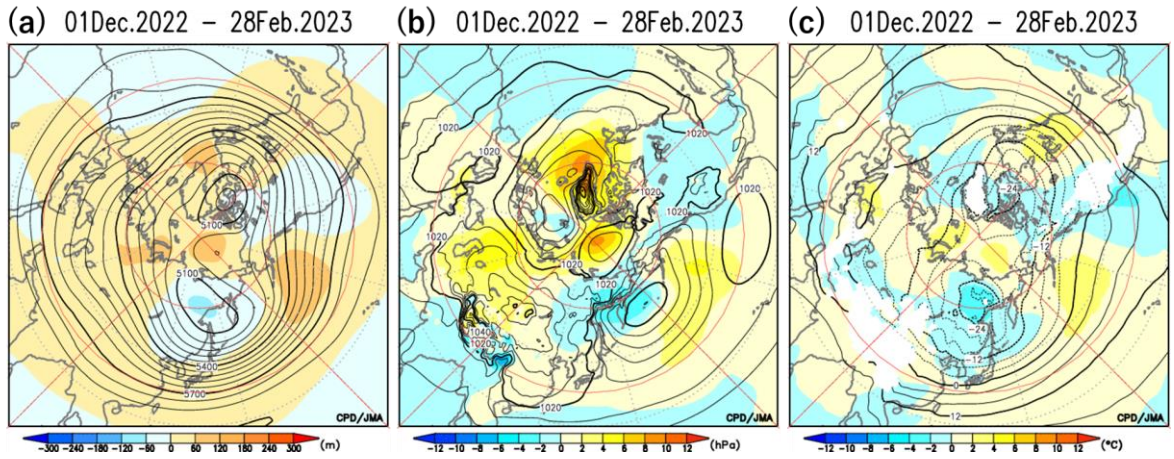

Figure 3-6 Three-month mean (a) 500-hPa height, (b) sea level pressure, and (c) 850-hPa temperature in winter 2022/2023

The contour intervals are (a) 60 m, (b) 4 hPa, and (c) 4 °C. The shading denotes related anomalies.

2.3 Cold spell events in East Asia

Several cold spells hit East Asia during winter, as partially manifested in monthly temperature anomalies (Figure 3-1). For instance, in the second half of December, the tropospheric polar vortex split in association with a blocking high to the north of Eastern Siberia, with one split part moving southward to the north of Japan (Figure 3-7 (b)) and bringing intense cold air masses from Central/Eastern Siberia to a wide area of East Asia (Figure 3-7 (c)). Meanwhile, as inferred from Figure 3-7 (a), the STJ over southern Eurasia exhibited an undulating structure with a southward meander over and around East Asia, which was favorable for southward cold-air inflow to the region. Such STJ meandering is partly attributable to enhanced convective activity in the area from the eastern tropical Indian Ocean to Indonesia. The blocking ridge to the north of Eastern Siberia may also be related to this anomalous convection. Such enhanced convective activity (a key factor in the below-normal temperature event over East Asia) was likely intensified by the Madden-Julian Oscillation (Madden and Julian 1971, 1972) in addition to the persistent La Niña conditions.

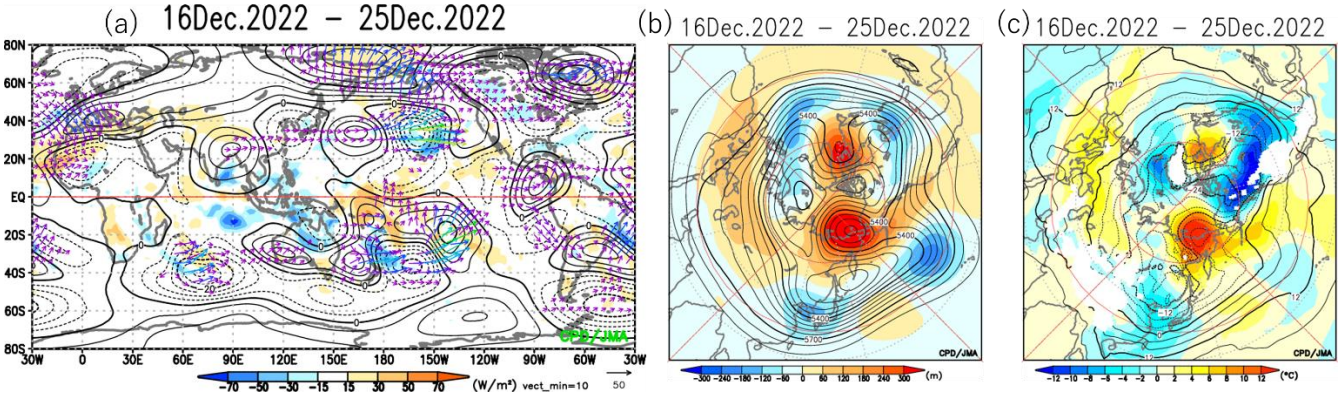

Figure 3-7 10-day mean (a) 200-hPa stream function anomalies, (b) 500-hPa height and (c) 850-hPa temperature from 16th to 25th December 2022

(a): The contours indicate stream function anomalies at intervals of 3×10^6 m^2/s, and the shadings show OLR anomalies [W/m^2]. The vectors denote horizontal component of wave activity flux [m^2/s^2] defined by Takaya and Nakamura (2001). (b) and (c): The contour intervals are (b) 60 m and (c) 4 °C. The shading denotes related anomalies.

(SATO Hirotaka, Tokyo Climate Center)

References

Kurihara, Y., T. Sakurai, and T. Kuragano, 2006: Global daily sea surface temperature analysis using data from satellite microwave radiometer, satellite infrared radiometer and in-situ observations. *Weather Service Bulletin*, **73**, Special issue, s1-s18 (in Japanese).

Kobayashi, S., Y. Kosaka, J. Chiba, T. Tokuhiro, Y. Harada, C. Kobayashi, and H. Naoe, 2021: JRA-3Q: Japanese Reanalysis for Three Quarters of a Century. *Joint WCRP-WWRP Symposium on Data Assimilation and Reanalysis/ECMWF Annual Seminar 2021*, online, 13-17 September 2021, O4-2.

Liebmann, B., and C. A. Smith, 1996: Description of a complete (interpolated) outgoing longwave radiation dataset. *Bull. Amer. Meteor. Soc.*, **77**, 1275–1277.

Madden, R.A. and P. R. Julian, 1971: Detection of a 40-50 day oscillation in the zonal wind in the tropical Pacific. *J. Atmos. Sci.*, **28**, 702-708.

Madden, R.A. and P. R. Julian, 1972: Description of global scale circulation cells in the tropics with a 40-50 day period. *J. Atmos. Sci.*, **29**, 1109-1123.

Takaya, K., and H. Nakamura, 2001: A formulation of a phase-independent wave-activity flux for stationary and migratory quasigeostrophic eddies on a zonally varying basic flow, *J. Atom. Sci.*, **58**, 608–627.

Wallace, J, M., and D. S. Gutzler, 1981: Teleconnections in the geopotential height field during the Northern Hemisphere winter, *Mon. Wea. Rev.*, **109**, 784–812.

Watanabe, M., and M. Kimoto, 2000: Atmospheric-ocean thermal coupling in the North Atlantic: A positive feedback. *Quart. J. Roy. Meteor. Soc.*, **126**, 3343–3369.

Watanabe, M., and M. Kimoto, 2001: Corrigendum. *Quart. J. Roy. Meteor. Soc.*, **127**, 733–734.

<<Table of contents <Top of this article

Commencement of JRA-3Q utilization in diagnosis products and iTacs

Reanalysis plays a crucial role in JMA's climate services and related activities (such as climate monitoring, seasonal forecast modeling and associated climate research) by providing long-term high-quality climate data. To further improve the quality of reanalysis data, JMA has developed the Japanese Reanalysis for Three Quarters of a Century (JRA-3Q) dataset, in which many of the deficiencies of the previous JRA-55 dataset are alleviated. JRA-3Q provides high-quality homogeneous reanalysis data covering the period from September 1947 onward, thereby extending the period of data coverage.

1. JRA-3Q outline (Table 4-1)

JMA's third Japanese global reanalysis, known as JRA-3Q, provides a comprehensive atmospheric dataset suitable for analysis of climate change and multi-decadal variability (Kobayashi et al. 2021) from September 1947 onward, thereby extending the previous period of data coverage. The data assimilation system for JRA-3Q is based on JMA's operational data assimilation system (as of December 2018), which has been extensively improved since the JRA-55 (Kobayashi et al. 2015) dataset was produced. The SST specified as the lower boundary condition for the forecast model is the Merged Satellite and In-Situ Data Global Daily Sea Surface Temperature (MGDSST; Kurihara et al. 2006) value based on observations made since June 1985 and Centennial In Situ Observation-based Estimates of the Variability of SSTs and Marine Meteorological Variables Version 2 (COBE-SST2; Hirahara et al. 2014) covering the period up to May 1985. For details of JRA-3Q, see the JRA-3Q comprehensive report (submitted to the Journal of the Meteorological Society of Japan).

	JRA-55	JRA-3Q
Version	Operational as of December 2009	Operational as of December 2018
Resolution	TL319 L60 (– 55 km); top layer at 0.1 hPa	TL479 L100(– 40 km); top layer at 0.01 hPa
Analysis scheme	4D-Var with T106 inner resolution	4D-Var with TL319 resolution
SST and sea ice	COBE-SST (1 degree)	Until May 1985: COBE-SST2 (1 degree) From June 1985 onward: MGDSST (0.25 degrees)

Table 4-1 JRA-55 and JRA-3Q data assimilation systems

2. Data assimilation system basics (Figure 4-1)

Figure 4-1 shows a time-series representation of root mean square (RMS) errors for two-day forecasts of geopotential height at 500 hPa averaged over the extratropical Northern and Southern Hemispheres. The increased forecast scores from JRA-25 (Onogi et al. 2007) to JRA-55 to JRA-3Q shown in Figure 4-1 indicate a steady improvement in the performance of the JMA data assimilation systems. JRA-3Q scores for the Northern Hemisphere are particularly stable, indicating high temporal consistency in the region (Figure 4-1 (a)). RMS errors for geopotential height at 500 hPa estimated in JRA-3Q were also significantly lower in the extratropical Southern Hemisphere during the 1990s (Figure 4-1 (b)).

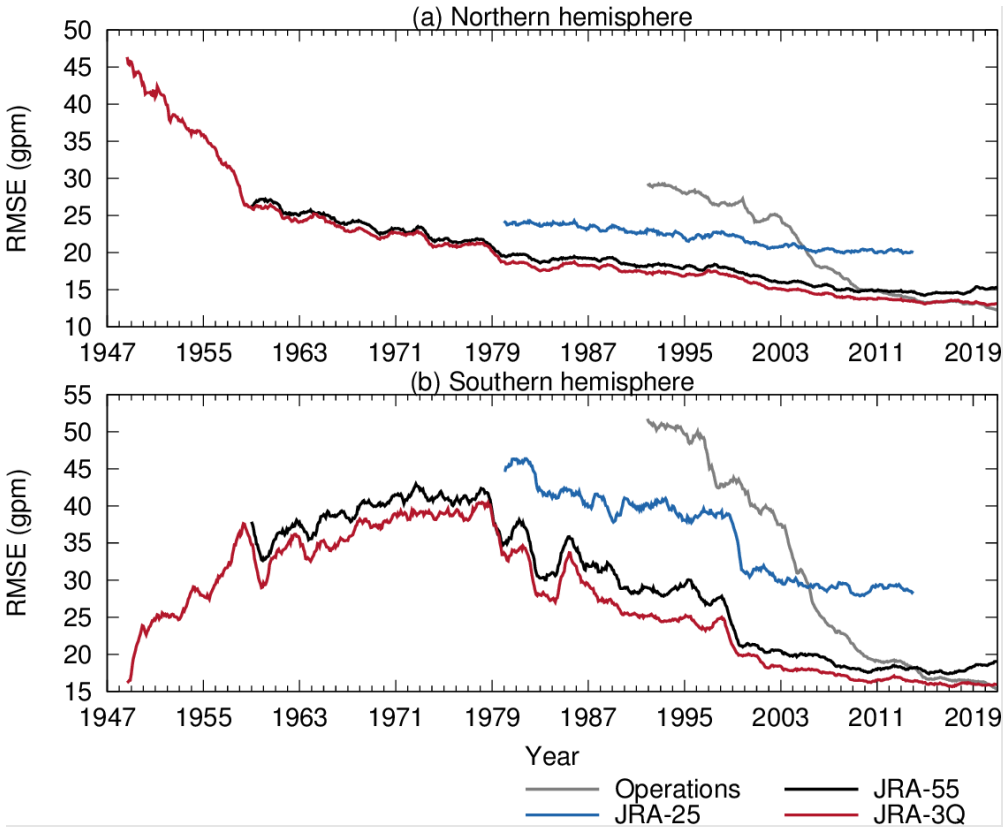

Figure 4-1 Time-series representation of RMS errors in two-day forecasts of 500-hPa geopotential height verified against own analysis in the extratropical (a) Northern and (b) Southern Hemispheres

3. TCC website and tool updates

Figures and tables for climate monitoring in the Climate Monitoring System and on the El Niño monitoring pages on the TCC website were replaced with data based on JRA-3Q and MGDSST/COBE-SST2 at the end of May 2023. There are no major differences in the characteristics of atmospheric circulation fields and sea surface temperature, while there is a slight difference in the duration of El Niño and La Niña events as defined by JMA. The content of the Impacts of El Niño/La Niña and Indian Ocean Dipole Events on the Global Climate page has also been replaced with new statistics based on JRA-3Q and indices from MGDSST/COBE-SST2. TCC has additionally updated the interactive Tool for Analysis of the Climate System (iTacs) in relation to the utilization of JRA-3Q and MGDSST/COBE-SST2. iTacs users can now access the new datasets.

4. Product availability

The JRA-3Q product is available for non-commercial purposes from the Data Integration & Analysis System (DIAS; https://jra.kishou.go.jp/JRA-3Q/index_en.html#MIRROR).

Reference

Hirahara, S., M. Ishii, and Y. Fukuda, 2014: Centennial-scale sea surface temperature analysis and its uncertainty. J. Climate, 27, 57–75.

Kobayashi, S., Y. Ota, Y. Harada, A. Ebita, M. Moriya, H. Onoda, K. Onogi, H. Kamahori, C. Kobayashi, H. Endo, K. Miyaoka, and K. Takahashi, 2015: The JRA-55 Reanalysis: General specifications and basic

characteristics. J. Meteor. Soc. Japan, 93, 5-48, doi:10.2151/jmsj.2015-001.

Kobayashi, S., Y. Kosaka, J. Chiba, T. Tokuhiro, Y. Harada, C. Kobayashi, and H. Naoe, 2021: JRA-3Q: Japanese Reanalysis for Three Quarters of a Century. Joint WCRP-WWRP Symposium on Data Assimilation and Reanalysis/ECMWF Annual Seminar 2021, online, 13-17 September 2021, O4-2.

Kurihara, Y., T. Sakurai, and T. Kuragano, 2006: Global daily sea surface temperature analysis using data from satellite microwave radiometer, satellite infrared radiometer and in-situ observations. Weather Service Bulletin, JMA, 73 , Special issue, s1–s18 (in Japanese).

Onogi, K., J. Tsutsui, H. Koide, M. Sakamoto, S. Kobayashi, H. Hatsushika, T. Matsumoto, N. Yamazaki, H. Kamahori, K. Takahashi, S. Kadokura, K. Wada, K. Kato, R. Oyama, T. Ose, N. Mannoji and R. Taira (2007): The JRA-25 Reanalysis. J. Meteor. Soc. Japan, 85, 369-432.

(ITO Akira, Tokyo Climate Center)

<<Table of contents <Top of this article

TCC and WMC Tokyo co-contributions to Regional Climate Outlook Forums

WMO Regional Climate Outlook Forums (RCOFs) bring together national, regional and international climate experts on an operational basis to produce regional climate outlooks based on input from participating NMHSs, regional institutions, Regional Climate Centres (RCCs) and global producers of climate predictions. By providing a platform for countries with similar climatological characteristics to discuss related matters, these forums ensure consistency in terms of access to and interpretation of climate information.

In spring 2023, representatives from TCC and the World Meteorological Centre (WMC) Tokyo attended:

- the 25th summer session of the South Asian Climate Outlook Forum (SASCOF-25)
- the 19th session of the Forum on Regional Climate Monitoring, Assessment and Prediction for Regional Association II (FOCRA II-19)

SASCOF-25

SATO Hitoshi from WMC-Tokyo provided summer season outlooks, including probabilistic forecasts, based on JMA's dynamical seasonal ensemble prediction system, and outlined Copernicus Climate Change Service (C3S) multi-model ensemble prediction, which the Japan Meteorological Agency (JMA) has engaged in since October 2020.

FOCRAII-19

IWAHIRA Tomoya and NATORI Hiroaki from TCC reported the results of climatic state monitoring for winter 2022/23 and provided outlooks, including probabilistic forecasts (as in SASCOF-25) at this meeting in Nanning, China. This was the first in-person gathering since 2019, with an online hybrid contingent.

Photo courtesy of CMA

These activities are intended to support the output of country-scale outlooks by National Meteorological and Hydrological Services (NMHSs), contribute to the summarization of consensus outlooks, and reduce climate disaster risk in the water, agriculture and health sectors for each target area. TCC and WMC-Tokyo are committed to collaboration with operational climate communities to enhance progress in forecast skill and application of climate information toward the resolution of common issues and realization of resilience to climate issues worldwide.

(TAKAHASHI Kiyotoshi, Tokyo Climate Center)

<<Table of contents <Top of this article

You can also find the latest newsletter from Japan International Cooperation Agency (JICA).

JICA Magazine

https://jicamagazine.jica.go.jp/en/

"JICA Magazine" is a public relations magazine published by JICA. It introduces the current situation of developing countries around the world, the people who are active in the field, and the content of their activities.

Any comments or inquiry on this newsletter and/or the TCC website would be much appreciated.

Please e-mail to tcc@met.kishou.go.jp.

(Editors: NEMOTO Noboru, TAKAHASHI Kiyotoshi)

Tokyo Climate Center, Japan Meteorological Agency
3-6-9 Toranomon, Minato City, Tokyo 105-8431, Japan

TCC Website:

https://www.data.jma.go.jp/tcc/tcc/index.html

<Top of this article